

A low volume 3D-printed temperature-controllable cuvette for UV visible spectroscopy

Jelena Pisaruka¹, Marcus K. Dymond^{1*}

¹Division of Chemistry, School of Pharmacy and Biological Sciences, University of Brighton, Huxley Building, Lewes Rd, Brighton, BN2 4GL, UK

* Author for correspondence: M.Dymond@brighton.ac.uk

Abstract

We report the fabrication of a 3D-printed water-heated cuvette that fits into a standard UV visible spectrophotometer. Full 3D-printable designs are provided and 3D-printing conditions have been optimised to provide options to print the cuvette in either acrylonitrile butadiene styrene or polylactic acid polymers, extending the range of solvents that are compatible with the design. We demonstrate the efficacy of the cuvette by determining the critical micelle concentration of sodium dodecyl sulphate at 40°C, the molar extinction coefficients of cobalt nitrate and *dsDNA* and by reproducing the thermochromic UV visible spectrum of a mixture of cobalt chloride, water and propan-2-ol.

In recent years there has been a rapid expansion in the number and quality of commercially available, affordable, fused deposition modelling (FDM) 3D-printers. These FDM 3D-printers allow end users to design, test and construct bespoke 3D-fabricated plastic prototypes targeted to their own individual applications [1]. Researchers in the chemical and biomedical sciences have made bespoke integrated reactionware [2–7], DNA adhesives [8], inserts for cuvettes [9] or X-ray absorption spectroscopy [10] that enable spectroelectrochemistry to be performed, surgical models and synthetic organs [11] and microfluidic pumps [12]. However, whilst there are a significant number of recent research success stories demonstrating the potential applications of 3D-printers, a number of key challenges remain. In particular the additive manufacturing process of FDM printing has a tendency to create small gaps between successive extruded layers, meaning 3D-prints are not always air or watertight. This is a particular challenge for FDM 3D-printing in milli or microfluidic applications where the pressure in the device is increased. Strategies for solving this leakage problem differ, one approach is to construct devices with increased wall thicknesses, typically 4 mm [3], although this does impose a lower limit on the size of device that can be constructed. Alternatively, recent work [13] has shown that many of these printing imperfections in ABS prints can be removed with acetone and that 3D-prints treated in this way, post production, have potential uses in fluid handling on a variety of scales.

Here we report our recent success using FDM 3D-printing to develop an inexpensive water heated UV visible cuvette made from ABS or PLA, which fits into a standard UV visible spectrometer.

UV visible spectroscopy was performed on a dual beam Shimadzu Corporation UV-2410PC spectrometer equipped with a single monochromator. BRAND® disposable polystyrene cuvettes (Sigma-Aldrich UK) were used for control studies. Cobalt nitrate, sodium dodecyl sulphate (SDS) and *ds*DNA from salmon sperm were purchased from Sigma- Aldrich UK. Cobalt chloride was purchased from ACROS organics UK and acetone, propan-2-ol and methylene blue were purchased from Fisher Scientific UK. A REFCO (-1 to 3 Bar; class 1.6) pressure gauge and OMEGA® OM-EL-USB-TC thermocouple USB datalogger were used to measure pressure and temperature respectively. 3D-printing was performed on a Makerbot Replicator 2X 3D printer (Makerbot Industries), 1.75 mm diameter ABS and PLA filaments were manufactured by Eliphilament and Makerbot Industries respectively. Prior to printing the build platform was covered with ScotchBlue™ adhesive tape for optimal adherence of the 3D-print. 3D-prints were designed in Autodesk123 and exported as STL files into Makerbot Desktop for slicing. The final optimised 3D printing settings for ABS and PLA are summarised in Tables S1 and S2 and fully printable designs are included as supporting information.

The UV visible spectrometer that we used was configured to accept standard 12 x 12 x 45 mm (width x depth x height) cuvettes; the incident beam centre was 15mm from the bottom of the cuvette, and the 1 mm polystyrene walls leave a sample path length of 10mm. Therefore our water heated cuvette needed the following design criteria to function effectively.

1. Sample path length of 10 mm
2. Sample centre 15 mm above the cuvette base.
3. Complete design no bigger than 12 x 12 mm (width x depth) and around 45 mm in height
4. Watertight

CAD designs of our 3D-printed water heated cuvette are shown in Figure 1A; we solved a number of problems before coming up with the final working cuvette. The most significant challenge encountered was leaking, either from the water-jacket chamber or the sample chamber. The origin of these leaks was two-fold, firstly small defects between layers resulting from the FDM printing process. Secondly, at printed vertices in the horizontal and vertical planes, sagging of the horizontal printed surface resulted in small voids, which leak. As noted, small defects can be fused using organic solvents [13], however bigger defects at vertices require carefully designed 3D-prints. A key design feature of our cuvette, which prevented sagging in the horizontal plane, was the inclusion of an inverted pyramid structure beneath the sample chamber, as noted in Figure 1B. The minimum and maximum sample volumes of the cuvette are 0.24 and 0.68 ml respectively.

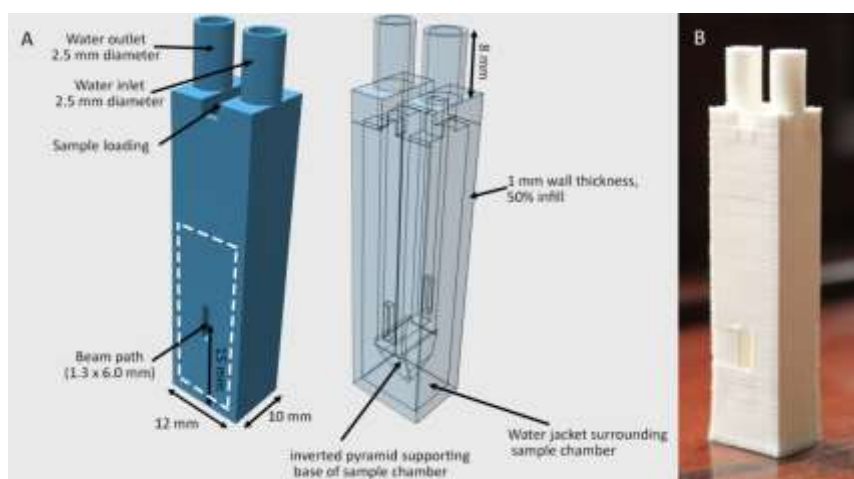


Figure 1A 3D-printed water heated cuvette, showing key dimensions and design features. The white dashed box indicates the approximate location of where optically transparent polystyrene, cut from polystyrene cuvettes was glued. Figure 1B shows a photograph of final cuvette printed in PLA.

Freshly printed ABS cuvettes were immersed in acetone (*circa* 20°C) and freshly printed PLA cuvettes were immersed in chloroform (*circa* 20°C) for 8 seconds to fuse defects between the printed layers. Excess solvent was removed and the cuvettes were dried in a fume hood for 2 hours before optically transparent plastic, cut from disposable polystyrene cuvettes, was glued to the faces of the printed cuvette, Figure 1A. To make the sample chamber watertight a slurry of ABS in acetone or PLA in chloroform was used as the glue. This provides an optical quality plastic, which cannot be 3D-printed. For studies utilising *ds*DNA we extended the working wavelength range of the cuvette by gluing on quartz slides using Gorilla™ super glue adhesive. This particular product was chosen due to it retaining strength at 100°C. After drying, cuvettes were pressure-tested to approximately 200 kPa by connecting the water input to a plastic syringe and sealing the output. Only cuvettes that passed this pressure test were used in subsequent studies, where they were connected to a recirculating water bath and fitted into the UV visible spectrometer. It should be noted that 8 seconds immersion in organic solvent was optimal and less than 1 in 5 cuvettes failed the pressure test. However it is likely that ambient temperature and the initial resolution of the 3D print will affect success rates.

To ascertain how long samples would need to be equilibrated for during measurements, we characterised the heating rate of the cuvette. This was achieved by attaching the thermocouple

probe the internal walls of the cuvette sample chamber. From an ambient water temperature of 17°C up to a maximum working temperature of 65°C, the glass transition temperature of PLA, the water bath heated linearly at a rate of $0.033 \pm 0.001^\circ\text{Cs}^{-1}$. Over the same temperature range the cuvette connected to the water bath heated linearly at $0.031 \pm 0.001^\circ\text{Cs}^{-1}$ indicating no significant lag between the water bath and cuvette heating. As a precaution samples were left to equilibrate at a constant temperature for 5 minutes prior to measurement of their absorbance.

Using both disposable polystyrene cuvettes and our 3D-printed cuvette we determined the value of the molar extinction coefficient (ϵ) for $\text{Co}(\text{NO}_3)_2$, at 510 nm, to be $480 \pm 10 \text{ m}^2\text{mol}^{-1}$ in water, indicating that the 3D-printed cuvette makes measurements as accurately as disposable plastic cuvettes. Figure S1A shows a plot of absorbance versus concentration for solutions of $\text{Co}(\text{NO}_3)_2$ determined in the 3D printed cuvette at room temperature.

As a further test we determined ϵ , at 260nm, of *ds*DNA from salmon sperm in the 3D-printed cuvette (with quartz covers glued to the sample chamber) at room temperature and compared it to the value we calculated using quartz cuvettes. Both sets of cuvettes gave molar extinction coefficients of *ds*DNA of $0.025 \pm 0.0005 (\mu\text{g}/\text{ml})^{-1} \text{ cm}^{-1}$. The ratio of absorbance at 260 and 280 ($A_{260/280}$), a measure of the protein contamination in DNA, was 1.81 ± 0.01 for both cuvette systems. Indicating that the 3D-printed cuvette with quartz covers also gives reproducible results when compared to the data obtained in quartz cuvettes. Figure S2A shows a plot of DNA absorbance at 260 nm versus concentration determined in the 3D-printed cuvette and Figure S2B shows the UV visible spectral plots of DNA from 200 to 400 nm at a range of concentrations obtained in the 3D-printed cuvette.

The next test we performed was to calculate the critical micelle concentration (CMC) of an amphiphile at an elevated temperature. We chose this test because phospholipids are amphiphiles and their critical aggregation concentration is important for biological processes, thus it is useful to measure this property at elevated temperature. However there are relatively few measurements of phospholipid CMC values in the literature and therefore for a more robust test we chose to determine the CMC of SDS, a commonly used anionic surfactant. The CMC of SDS has been determined many times in the literature using a number of different methods. In water at 25°C measurements of the CMC of SDS range from 8.3 mM [14] using capillary electrophoresis, 8.3 mM using a temperature shock method in combination with the dye acridine orange and UV visible spectroscopy, $8.1 \pm 0.12 \text{ mM}$ to 7.0 mM [15] by conductance measurements [16] and titration calorimetry [17]. The CMC of SDS shows slight temperature dependence with literature values at 30°C in water of $7.3 \pm 0.3 \text{ mM}$ [18] and 7.2 mM at 40°C and a general decrease in CMC with increasing temperature [19].

Using a UV visible method in combination with the dye methylene blue, such that the dye partitions into the interior of micelles changing the concentration of the dye in solution, we determined the CMC of SDS at 40°C to be $7.0 \pm 0.3 \text{ mM}$ in water, which agrees well with measurements in the literature. Figure S1B shows the results of this analysis, where the CMC is estimated from the graph by considering the gradients of two intersecting lines [20], which correspond to the linear increase in absorbance of the dye as a function of concentration in the presence and absence of micelles. There are a number of reports in the literature where the CMC of different amphiphiles, i.e. surfactants or phospholipid analogues, have been determined at 37°C, which is particularly relevant for

applications in biological systems [21]. We anticipate that this 3D-printed cuvette will be useful for these soft-matter applications.

As a final test we reproduced the thermochromic shift in the UV visible spectra of CoCl_2 solutions of water and propan-2-ol, which arise due to the different absorbance spectra of cobalt chloride complexes in tetrahedral or octahedral geometries. In the tetrahedral arrangement these complexes are pink in colour and in the octahedral form these complexes are blue in colour. In solutions of water and propan-2-ol, a temperature-dependence exists whereby the tetrahedral form, stable at low temperature, exists in equilibrium with the octahedral form, favoured at higher temperature. This effect is driven by different solvation arrangements of water and propan-2-ol molecules being favoured at different temperatures and hence a different coordination structure for the cobalt chloride salt [22]. The percentage of water in the solvent mixture dictates the temperature range over which the thermochromic behaviour is observed, with higher water fractions shifting the dependence to higher temperatures [23].

We measured the thermochromic behaviour of CoCl_2 solutions of water and propan-2-ol using our water heated cuvette and compared our spectra to those obtained by Dybko et al. [22] in a commercially available heated cuvette system. Figure 2 shows the temperature-dependence of the UV visible spectrum in the range of 400 to 800 nm for 10ml saturated CoCl_2 in water added to 40 ml propan-2-ol.

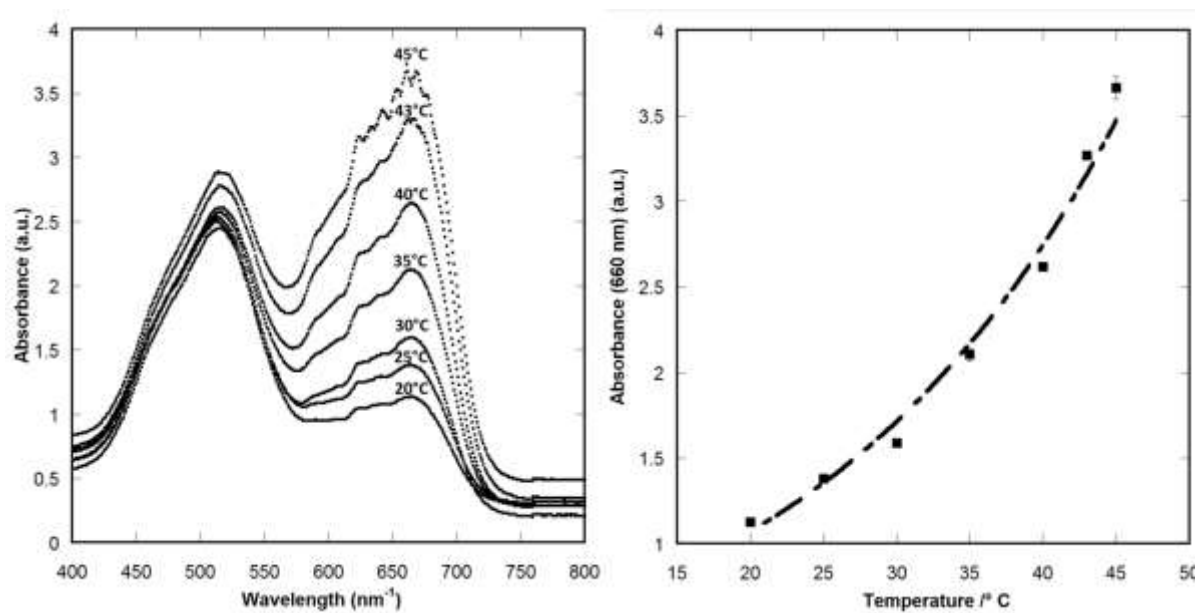


Figure 2A the thermochromic shift of UV visible spectra for CoCl_2 in solutions of water and propan-2-ol. Measurements were made at water bath temperatures of 20, 25, 30, 35, 40, 43 and 45°C, the peak centred at 660 nm increases in size with temperature. Figure 2B dependence of absorption at 660 nm on temperature for CoCl_2 solutions in solutions of water and propan-2-ol. Absorbance data were extrapolated from Figure 2A (at 660 nm), the dashed line shows an exponential line of best fit over the temperature range studied ($y = 0.42 \times e^{(0.047x)}$, $R^2 = 0.99$).

The results we obtain in Figure 2A show identical trends to those reported in the literature [22], with one peak centred around 525 nm and the emergence of a second peak in the range of 600 to 700 nm with increasing temperature, corresponding to the octahedral cobalt complex. The maximum wavelength (λ_{max}) of absorbance of the octahedral complex is 660 nm, which increases in absorbance intensity as the solution temperature is increased. The relationship between temperature and absorbance follows a sigmoidal dependence [22], rather than the linear dependence observed for concentration versus absorbance. Figure 2B shows the temperature dependence of the absorbance at 660 nm determined in our 3D-printed cuvette also showing the trend reported by Dybko et al. [22].

We have 3D-printed and tested a water heated cuvette for UV visible spectroscopy, demonstrating that the 3D-printed cuvette provides reproducible temperature dependent spectra when compared to disposable cuvettes, quartz cuvettes and literature studies. We constructed our cuvette from both ABS and PLA polymers making versions with 'windows' made from optically transparent polystyrene or quartz slides. The print reproducibility was greater for the cuvette constructed from PLA but the lower glass transition temperature of PLA (*circa* 65°C) means that PLA cuvettes have a lower working range when compared to cuvettes made ABS (glass transition temperature *circa* 105°C). PLA has different solvent compatibility [24] to ABS and is thus better suited for obtaining UV visible spectra in a range of organic solvents although both cuvettes can be used for water-based studies. The beam centre on our spectrophotometer was 15mm, whilst this is almost standard, our design can be modified for spectrometers with different beam centre heights. The material cost of producing the cuvette is around £0.10 pounds sterling and subject to the constraints of dimension it is likely that these cuvettes are compatible with microelectrodes further extending the range of applications. In particular we foresee that this cuvette is ideal for preliminary research work, when conventional heated UV visible machines are not available, and for educational users.

Acknowledgements

The authors thank Lisa O'Rourke for proof-reading the document. This work was supported by the School of Pharmacy and Biological Sciences, University of Brighton who provided start-up funding for MKD to purchase the 3D-printer.

References

- [1] C. Schubert, M.C. van Langeveld, L.A. Donoso, Innovations in 3D printing: a 3D overview from optics to organs, *Br. J. Ophthalmol.* (2013) 159–161. doi:10.1136/bjophthalmol-2013-304446.
- [2] P.J. Kitson, M.H. Rosnes, V. Sans, V. Dragone, L. Cronin, Configurable 3D-Printed millifluidic and microfluidic “lab on a chip” reactionware devices, *Lab Chip.* 12 (2012) 3267. doi:10.1039/c2lc40761b.
- [3] P.J. Kitson, R.J. Marshall, D. Long, R.S. Forgan, L. Cronin, 3D Printed High-Throughput Hydrothermal Reactionware for Discovery, Optimization, and Scale-Up, *Angew. Chemie Int. Ed.* 53 (2014) 12723–12728.
- [4] G. Chisholm, P.J. Kitson, N.D. Kirkaldy, L.G. Bloor, L. Cronin, 3D printed flow plates for the electrolysis of water: an economic and adaptable approach to device manufacture, *Energy Environ. Sci.* 7 (2014) 3026–3032. doi:10.1039/c4ee01426j.
- [5] P.J. Kitson, M.D. Symes, V. Dragone, L. Cronin, Combining 3D printing and liquid handling to produce user-friendly reactionware for chemical synthesis and purification, *Chem. Sci.* 4 (2013) 3099–3103. doi:10.1039/c3sc51253c.
- [6] J.S. Mathieson, M.H. Rosnes, V. Sans, P.J. Kitson, L. Cronin, Continuous parallel ESI-MS analysis of reactions carried out in a bespoke 3D printed device, *Beilstein J. Nanotechnol.* 4 (2013) 285–291. doi:10.3762/bjnano.4.31.
- [7] V. Dragone, V. Sans, M.H. Rosnes, P.J. Kitson, L. Cronin, 3D-printed devices for continuous-flow organic chemistry, *Beilstein J. Org. Chem.* 9 (2013) 951–959. doi:10.3762/bjoc.9.109.
- [8] P.B. Allen, Z. Khaing, C.E. Schmidt, A.D. Ellington, 3D Printing with Nucleic Acid Adhesives, *ACS Biomater. Sci. Eng.* 1 (2015) 19–26.
- [9] J.M. Brisendine, A.C. Mutter, J.F. Cerda, R.L. Koder, A three-dimensional printed cell for rapid, low-volume spectroelectrochemistry, *Anal. Biochem.* 439 (2013) 1–3. doi:10.1016/j.ab.2013.03.036.
- [10] E. Achilli, A. Minguzzi, A. Visibile, C. Locatelli, A. Vertova, A. Naldoni, S. Rondinini, F. Auricchio, S. Marconi, M. Fracchia, P. Ghigna, 3D-printed photo-spectroelectrochemical devices for in situ and in operando X-ray absorption spectroscopy investigation, *J. Synchrotron Rad.* 23 (2016) 622–628.
- [11] S. V Murphy, A. Atala, 3D bioprinting of tissues and organs, *Nat. Biotechnol.* 32 (2014) 773–785.
- [12] D.J. Thomas, Z. Tehrani, B. Redfearn, 3-D printed composite microfluidic pump for wearable biomedical applications, *Addit. Manuf.* 9 (2016) 30–38. doi:10.1016/j.addma.2015.12.004.
- [13] E.J. McCullough, V.K. Yadavalli, Surface modification of fused deposition modeling ABS to enable rapid prototyping of biomedical microdevices, *J. Mater. Process. Technol.* 213 (2013) 947–954. doi:10.1016/j.jmatprotec.2012.12.015.
- [14] A. Cifuentes, J.L. Bernal, J.C. Diez-Masa, Determination of critical micelle concentration values using capillary electrophoresis instrumentation, *Anal. Chem.* 69 (1997) 4271–4274. doi:10.1021/ac970696n.
- [15] A. Fernández-Alonso, C. Bravo-Díaz, Effects of micellar aggregates on the kinetics and

- mechanism of the reaction between 4-nitrobenzenediazonium ions and some amino acids, *Helv. Chim. Acta.* 90 (2007) 1141–1151. doi:10.1002/hlca.200790113.
- [16] E. Fuguet, C. Ràfols, M. Rosés, E. Bosch, Critical micelle concentration of surfactants in aqueous buffered and unbuffered systems, *Anal. Chim. Acta.* 548 (2005) 95–100. doi:10.1016/j.aca.2005.05.069.
- [17] M.J. Blandamer, B. Briggs, P.M. Cullis, K.D. Irlam, J.B.F.N. Engberts, J. Kevelam, Titration microcalorimetry of adsorption processes in aqueous systems Interaction of sodium dodecylsulfate and sodium decylsulfate with poly(N-vinylpyrrolidone), *J. Chem. Soc. Faraday Trans.* 94 (1998) 259–266. doi:10.1039/a704667g.
- [18] W. Loh, L.A.C. Teixeira, L. Lee, Isothermal Calorimetric Investigation of the Interaction of Poly (N -isopropylacrylamide) and Ionic Surfactants, *J. Phys. Chem. B.* 108 (2004) 3196–3201. doi:10.1021/jp037190v.
- [19] N.S. Babu, Thermodynamic study of polymersurfactant interaction in aqueous system, *J. Indian Chem. Soc.* 83 (2006) 39 – 41.
- [20] A. Domínguez, A. Fernández, N. González, E. Iglesias, L. Montenegro, Determination of Critical Micelle Concentration of Some Surfactants by Three Techniques, *J. Chem. Educ.* 74 (1997) 1227–1231. doi:10.1021/ed074p1227.
- [21] M.K. Dymond, G.S. Attard, Cationic type I amphiphiles as modulators of membrane curvature elastic stress in vivo., *Langmuir.* 24 (2008) 11743–11751. doi:10.1021/la8017612.
- [22] A. Dybko, W. Wróblewski, E. Roźniecka, J. Maciejewski, Z. Brzózka, Comparison of two thermochromic solutions for fibre optic temperature probes, *Sensors Actuators, A Phys.* 76 (1999) 203–207. doi:10.1016/S0924-4247(99)00030-8.
- [23] K. Sone, Y. Fukuda, J. Mizusaki, K. Moriyama, Bemerkungen über Thermochromie von Kobalt (II) chloridlösungen in organischen Medien, 1. Mitt.: Lösungen in verschiedenen Alkoholen., *Monatshefte Für Chemie/Chemical Mon.* 107 (1976) 271–281.
- [24] S. Abbot, Chemical Compatibility of Poly(Lactic Acid): A Practical Framework Using Hansen Solubility Parameters, in: *Poly(Lactic Acid) Synth. Struct. Prop. Process. Appl.*, John Wiley & Sons, Inc., Hoboken, NJ., 2010: pp. 83–95. doi:10.1002/9780470649848.

Supporting Information: A low volume 3D-printed temperature-controllable cuvette for UV Visible spectroscopy

Jelena Pisaruka¹, Marcus K. Dymond^{1*}

¹Division of Chemistry, School of Pharmacy and Biological Sciences, University of Brighton, Huxley Building, Lewes Rd, Brighton, BN2 4GL, UK

* Author for correspondence: M.Dymond@brighton.ac.uk

Supplementary methodology

3D-printing conditions

During construction we trialled different infill densities before settling on a density of 50% for the final design, at lower infill densities (10%) we found the cuvette was fragile and distorted more easily during prolonged heating. Aside from danger of leakage, this distortion caused experimental artefacts when measuring the absorbance spectra of samples. At higher infill density, close to 100%, 3D-prints were stronger but distorted more during printing. In part this distortion was due to the extruded filament not cooling sufficiently before the next layer was added, thus as the printer extruder extrudes the current layer, layers below are slightly mobile. This problem can be eliminated by increasing the minimum layer duration, see Tables S1 and S2, in the print settings and tends to be related to the size of the structure being printed. It was particularly problematic when printing the small 2.5 mm diameter water inlet and water outlet. Our highest quality cuvettes were obtained by 3D-printing a monolith beside the cuvette, which gave each layer sufficient time to cool before the next was added. This approach also prevented the build-up of molten plastic on the extruder head which can result from extending the minimum layer duration.

Table S1. Optimal print settings for ABS cuvettes on the MakerBot Replicator 2X.

Extruder Temperature	245°C	Platform Temperature	110°C
Travel Speed	150 mm/s	Z-axis Travel Speed	23 mm/s
Minimum Layer Duration	5.0 s	First Layer Raft Print Speed	50 mm/s
Infill Print Speed	90 mm/s	Inserts Print Speed	90 mm/s
Outlines Print Speed	40 mm/s	Raft Print Speed	90 mm/s
Raft Base Print Speed	10 mm/s	Bridges Print Speed	40 mm/s
First Layer Print Speed	30 mm/s	Infill Density	50%
Infill Pattern	Hexagonal	Layer Height	0.20 mm
Infill Layer Height	0.20 mm	Number of Shells	2
Roof Thickness	0.80 mm	Floor Thickness	0.80 mm
Coarseness	0.0001 mm	Raft-Model Spacing	0.35 mm
Raft Margin	4.0 mm	Support	Off
Bridging	Off	Filament Diameter	1.77 mm
Retraction Distance	1.3 mm	Retraction Speed	25 mm/s
Restart Speed	25 mm/s	Extra Restart Distance	0.0 mm

Table S2. Optimal print settings for PLA cuvettes on the MakerBot Replicator 2X.

Extruder Temperature	220°C	Platform Temperature	110°C
Travel Speed	150 mm/s	Z-axis Travel Speed	23 mm/s
Minimum Layer Duration	5.0 s	First Layer Raft Print Speed	50 mm/s
Infill Print Speed	90 mm/s	Inserts Print Speed	90 mm/s
Outlines Print Speed	40 mm/s	Raft Print Speed	90 mm/s
Raft Base Print Speed	10 mm/s	Bridges Print Speed	40 mm/s
First Layer Print Speed	30 mm/s	Infill Density	50%
Infill Pattern	Hexagonal	Layer Height	0.20 mm
Infill Layer Height	0.20 mm	Number of Shells	2
Roof Thickness	0.80 mm	Floor Thickness	0.80 mm
Coarseness	0.0001 mm	Raft-Model Spacing	0.35 mm
Raft Margin	4.0 mm	Support	Off
Bridging	Off	Filament Diameter	1.77 mm
Retraction Distance	1.3 mm	Retraction Speed	25 mm/s
Restart Speed	25 mm/s	Extra Restart Distance	0.0 mm

Characterisation of the thermal sensitivity of the 3D-printed cuvette

The thermal sensitivity of the 3D-printed cuvette was determined to ensure that in experimental runs sufficient time would be left for samples to reach thermodynamic equilibrium. The heating rates of both the water bath and the 3D-printed cuvette were determined using a digital thermocouple, measuring the temperature at 30 second intervals.

Determination of the molar extinction coefficient of $\text{Co}(\text{NO}_3)_2$ in water

$\text{Co}(\text{NO}_3)_2$ solutions were prepared with concentrations of 0.025 M, 0.04 M, 0.05 M, 0.08 M, 0.10 M, 0.133 M and 0.20 M and their absorbance measured over the range 350 – 650 nm using water as a blank. Each concentration was measured in triplicate using disposable cuvettes or a water heated-printed cuvettes made from ABS and PLA and background subtracted using the appropriate cuvette containing water. The molar extinction coefficient (ϵ) was determined using the Beer-Lambert principle from linear fits to plots of the $\text{Co}(\text{NO}_3)_2$ concentration versus their absorbance at 510 nm, which yields ϵ_{510} as the function of the gradient of the line and the path length (10 mm), see Equation 1.

$$A = \epsilon cl \quad \text{Equation 1,}$$

Determination of the molar extinction coefficient of dsDNA in 50 mM Trizma buffer pH 7.4

In 50 mM Trizma buffer, dsDNA solutions were prepared with concentrations of 12.6, 23.9, 34.1, 43.3, 51.6 $\mu\text{g ml}^{-1}$ and their absorbance measured over the range 200 – 400 nm using 50 mM Trizma

buffer as a blank. Each concentration was measured in triplicate using quartz cuvettes or a water heated-printed cuvettes fitted with quartz covers made from ABS. The molar extinction coefficient (ϵ) was determined using the Beer-Lambert principle from linear fits to plots of the *ds*DNA concentration versus their absorbance at 260 nm, which yields ϵ_{260} as the function of the gradient of the line and the path length (10 mm), see Equation 1.

Determination of the CMC of SDS at 40°C

Ten solutions of SDS were prepared at 3 mM, 4 mM, 5 mM, 6 mM, 7 mM, 8 mM, 9 mM, 10 mM, 11 mM and 12 mM in water, containing 10^{-5} M methylene blue. The water heated cuvette was placed into the UV visible spectrometer and heated to 40°C before the background absorbance of 10^{-5} M methylene blue in water was recorded. Absorbance measurements were made in triplicate between 650 and 670 nm and in increasing SDS concentrations, allowing 5 minutes for samples to reach thermal equilibrium. Samples were removed from the cuvette using a glass pipette before rinsing with 10^{-5} M methylene blue in water, prior to the addition of the next sample. The CMC was determined using absorbance measurements at 660nm.

Determination of the thermochromic shift of mixtures of CoCl₂, water and propan-2-ol

10 ml of saturated aqueous CoCl₂ was added to 40mL of isopropyl alcohol as previously published [1]. The 3D-printed cuvette was connected to a water bath placed into the UV visible machine and mixture absorbance between 400 – 800 nm was measured at temperatures between 15°C - 45°C in increments, leaving 5 minutes for thermal equilibration between measurements.

Supplementary Figures

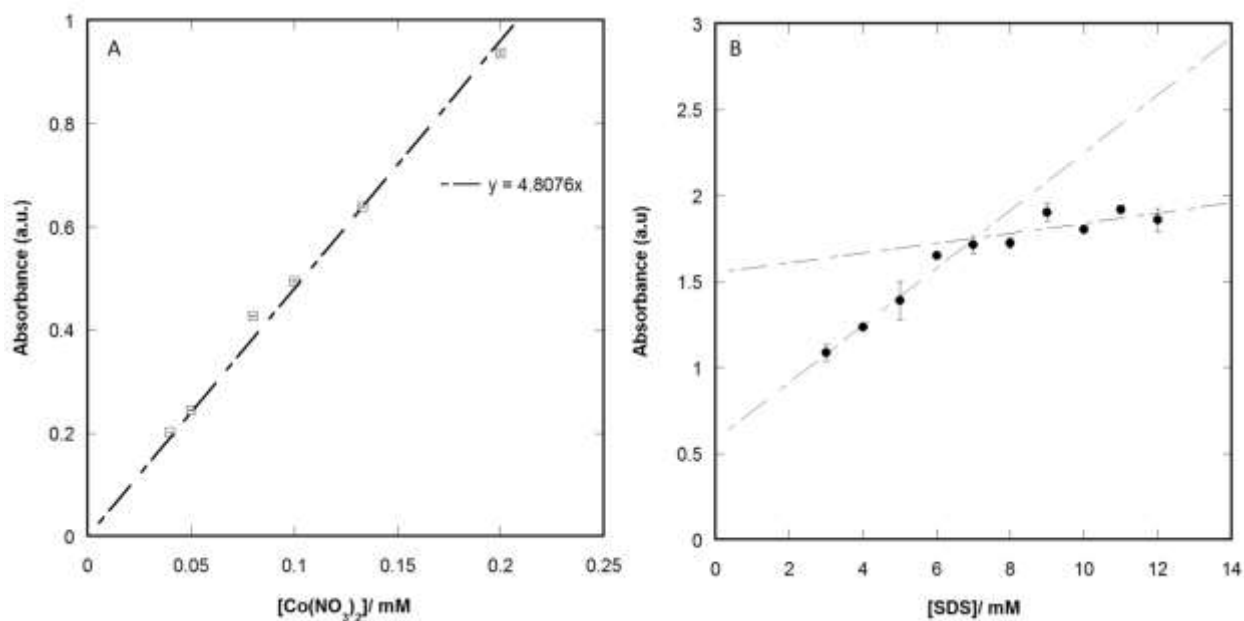


Figure S1A, the molar extinction coefficient determined for $\text{Co}(\text{NO}_3)_2$ at 510 nm and Figure S1B the CMC of SDS determined at 40°C using the low-volume 3D-printed cuvette. The CMC is determined from Figure S1B as the point where the two lines intersect.

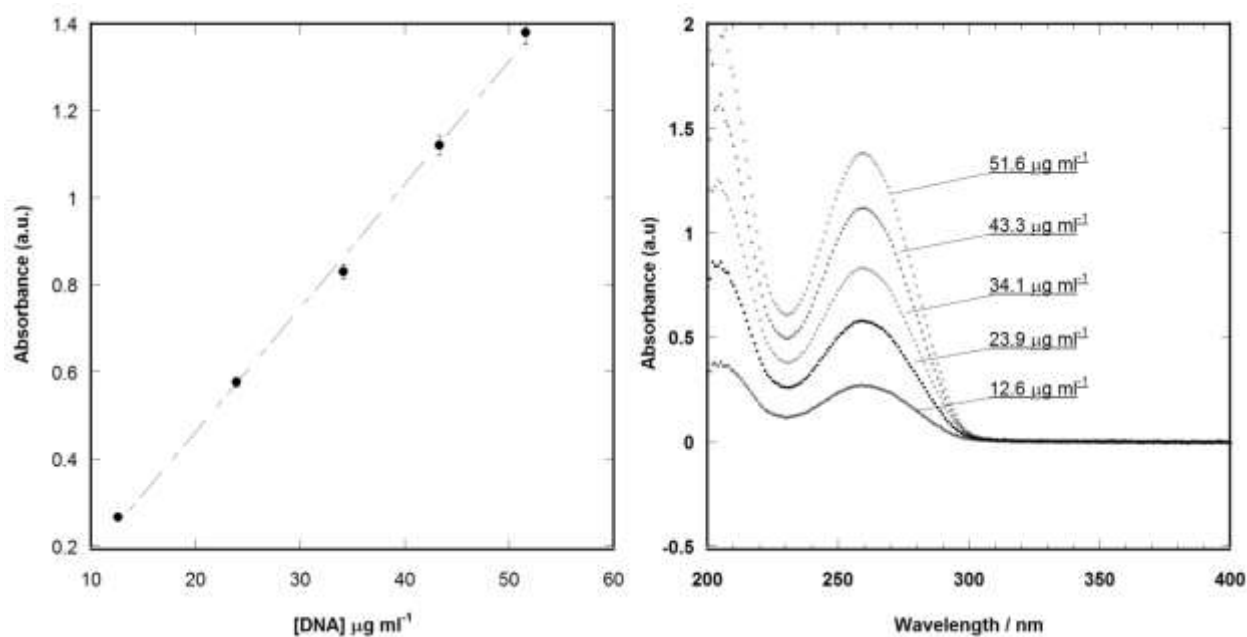


Figure S2A the molar extinction coefficient determined for *dsDNA* at 510 nm and Figure S2B, the absorbance spectrum of *dsDNA* from 200 to 400 nm at a range of concentrations. Spectra in both figures were obtained using the 3D-printed cuvette fitted with quartz covers.

- [1] A. Dybko, W. Wróblewski, E. Roźniecka, J. Maciejewski, Z. Brzózka, Comparison of two thermochromic solutions for fibre optic temperature probes, *Sensors Actuators, A Phys.* 76

(1999) 203–207. doi:10.1016/S0924-4247(99)00030-8.